Ultramicroscopy 40 (1992) 265–270
North-Holland

ultramicroscopy

# Morphology of silicon grain boundaries in Sr-modified Al–Si eutectic alloys by HREM

M Shamsuzzoha, P A Deymier
*Department of Materials Science and Engineering, University of Arizona, Tucson, AZ 85721, USA*

and

David J Smith
*Center for Solid State Science and Department of Physics, Arizona State University, Tempe, AZ 85287, USA*

Received 6 January 1991, at Editorial Office 28 August 1991

Crystallographic changes in the $\Sigma3\langle110\rangle/\{111\}$, $\Sigma3\langle110\rangle/\{112\}$ and $\Sigma9\langle110\rangle/\{112\}$ boundaries induced by the presence of strontium in the silicon phase of Sr-modified Al–Si alloys have been studied by high-resolution electron microscopy The $\Sigma3$ boundaries possessing {111} and {112} planes in the pure silicon phase often exhibit asymmetric morphologies in the Sr-modified phase Interaction of various $\Sigma3\langle110\rangle/\{111\}$ boundaries results in both $\Sigma3\langle110\rangle/\{112\}$ and $\Sigma9\langle110\rangle/\{112\}$ boundaries The resulting $\Sigma9$ boundaries also show asymmetrical inclination

## 1. Introduction

Impurities can have a very strong effect on the morphology of grain boundaries For example, it is well established that segregation at grain boundaries in a wide range of materials promotes the formation of new grain boundary configurations such as faceting [1–3] Unfortunately, very little is known about the crystallographic structure of chemically modified boundaries

Significant advances have been made towards understanding the atomic structure of grain boundaries in pure metals, ceramics and semiconductors For instance, determinations of the atomic structure of pure symmetrical-tilt high-angle coincident boundaries in silicon and germanium such as $\Sigma3\langle110\rangle/\{111\}$ [4], $\Sigma3\langle110\rangle/\{112\}$ [5] and $\Sigma9\langle110\rangle/\{112\}$ [6] by high-resolution electron microscopy (HREM) have firmly established that such boundaries assume a symmetric morphology in their equilibrium configuration Moreover, it is always possible to describe the boundaries in terms of simple structural units, and tetrahedral coordination is maintained everywhere so that there are no dangling bonds associated with the (periodic) structural units [6]

High-resolution electron microscopy can also be applied to obtain information about the structure and morphology of similar grain boundaries in doped Si Hence, we have recently directed our attention to Sr-impurity-induced morphological changes in $\Sigma3\langle110\rangle/\{111\}$, $\Sigma3\langle110\rangle/\{112\}$ and $\Sigma9\langle110\rangle/\{112\}$ grain boundaries in silicon using HREM This paper describes some high-resolution imaging of the morphological changes in grain boundaries present in the silicon phase of Sr-modified Al–Si eutectic alloys

## 2. Experiment

Al–12 7wt%Si eutectic alloys with 0 05% Sr were vacuum cast from Al and Si, each of 99 999%

0304-3991/92/$05 00 

purity, and Al–5wt%Si master alloys of 99 9% purity The cast billets were remelted and unidirectionally solidified at a rate of 50 $\mu$m s$^{-1}$ The thermal gradient at the solid–liquid interface was determined by prior calibration of the furnace apparatus and found to be 50°C cm$^{-1}$ Transverse and longitudinal section specimens taken from near the center of the solidified samples were used for thin-foil preparation The thin-foil specimens were prepared by a method described elsewhere [7], using electropolishing followed by ion-beam thinning Thin foils thus prepared were examined with a 120 kV Philips electron microscope and a 400 kV JEM-4000EX HREM High-resolution electron micrographs were recorded near the optimum defocus typically at a magnification of 500 000 times The pairs of Si atomic columns appeared black under these experimental conditions and the structure of simple silicon grain boundaries could be determined unambiguously

## 3. Experimental results

In transverse and longitudinal sections of eutectic Al–Si alloys, the silicon phase exhibits a fibrous morphology with the direction of the fiber axis ranging anywhere between ⟨100⟩ and ⟨110⟩ [8] Cozonal twin traces in the fibrous silicon were detected when the specimen was aligned with various ⟨110⟩ of the silicon crystals parallel to the electron beam Using the goniometer tilting facilities of the microscopes, the orientations of selected silicon fibers were shifted to ⟨110⟩ zone axes by centering the corresponding Kikuchi line patterns

A high-resolution image of a typical segment

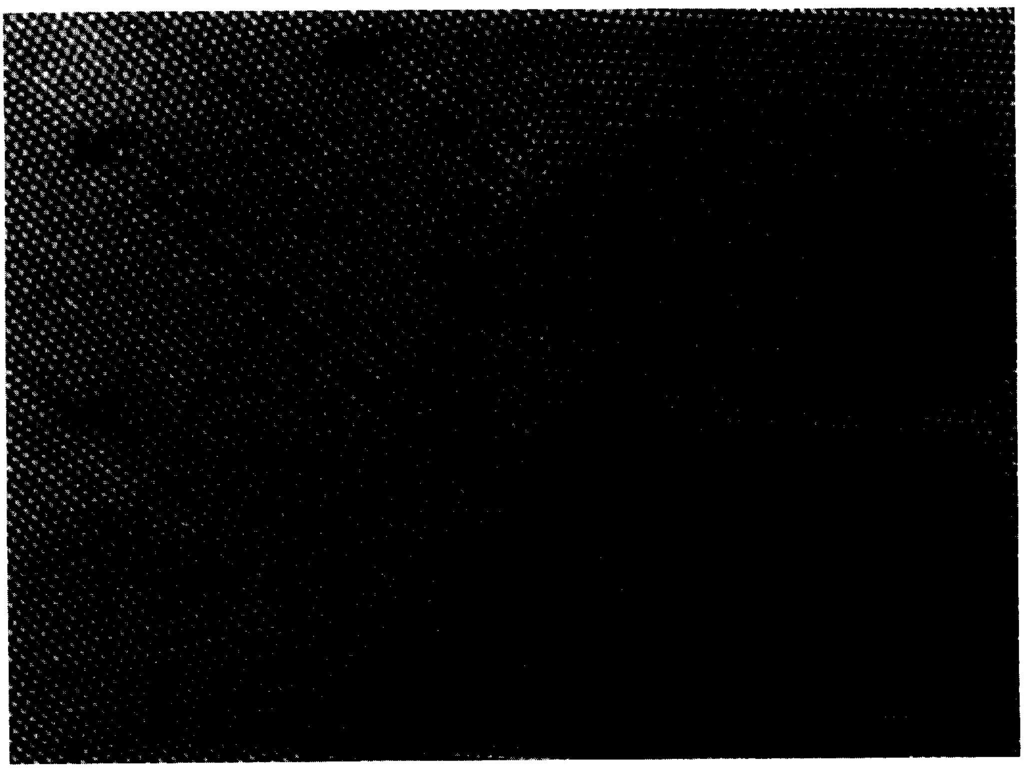

Fig 1 HREM image with incident beam parallel to {111} twinning plane of silicon fiber in Al–12 7% Si–0 05% Sr alloy

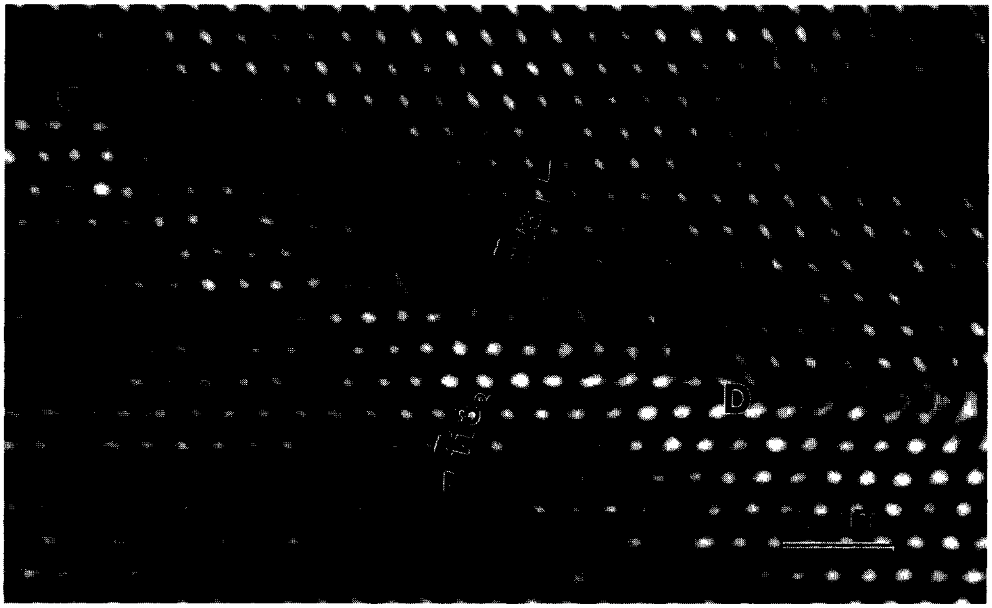

Fig 2 HREM image recorded along [110] direction of Si fiber showing an asymmetric portion of a $\Sigma 3$ boundary connecting two symmetric segments of $\Sigma 3[110]/(\bar{1}11)$ twin interface

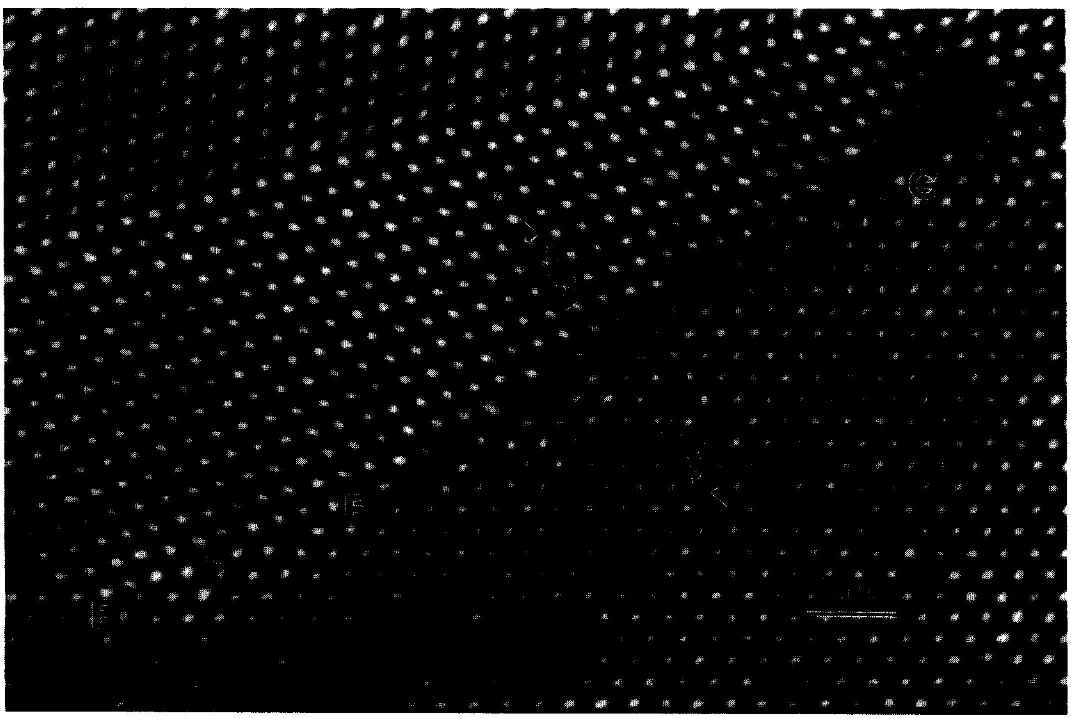

Fig 3 HREM image with incident beam parallel to {111} plane of Si fiber revealing an asymmetric $\Sigma 3[110]/(112)$ twin boundary

of silicon fiber taken with the electron beam closely aligned with a $\langle 110 \rangle$ direction of the fiber is shown in fig 1 The majority of Si grains in this micrograph show parallel $\Sigma 3$ twin (T) or microtwin (MT) boundaries with a 70 5° misorientation along the common $\langle 110 \rangle$ axis, and on two cozonal $\{111\}$ boundary planes extending along two different $\langle 112 \rangle$ directions Exceptions to these symmetric $\Sigma 3$ grain boundaries can be found in the micrograph at the positions marked A and B where a $\Sigma 3$ boundary possessing an asymmetric boundary plane is observed

The asymmetry is very clear in the micrograph of fig 2, taken from another silicon fiber under similar imaging conditions The $\Sigma 3$ boundary to the left of the position marked C and to the right of the position marked D exhibits a perfectly symmetric $\{111\}$ twin plane Whereas the boundary connecting these two locations is very asymmetric, the image of this region reveals the boundary plane to be roughly parallel to $\{113\}$ for the two crystals on either side of the boundary The $\{113\}$ boundary plane inclination is produced by a sequence of steps of height $\frac{1}{3}\langle 111 \rangle$

Further silicon fibers observed under similar experimental conditions also exhibit a number of other asymmetric $\Sigma 3$ and $\Sigma 9$ boundaries Fig 3 shows an asymmetric $\Sigma 3$ boundary located between the positions marked E and G The boundary is mainly comprised of two segments one section located between E and F has a boundary plane roughly parallel to $\{111\}_1$ and $\{113\}_2$, while the other segment lying between F and G is almost symmetric and runs approximately along $\{112\}$ of both crystals 1 and 2 An interesting feature of this partly symmetric and partly asymmetric boundary is the existence of a remarkable continuity of $\{111\}$ planes across the interface Contrary to this observation, the equilibrium structure of the $\Sigma 3\langle 110 \rangle/\{112\}$ boundary, as reported in the literature [9], has the $\{111\}$ planes across the $\{112\}$ boundary plane exhibiting a rigid-body displacement of $\frac{1}{6}\langle 111 \rangle$ along the boundary plane

The grain boundary in fig 4 is a typical asymmetric $\Sigma 9$ boundary This boundary is again comprised of two segments The boundary segment marked H and I in this figure has a boundary

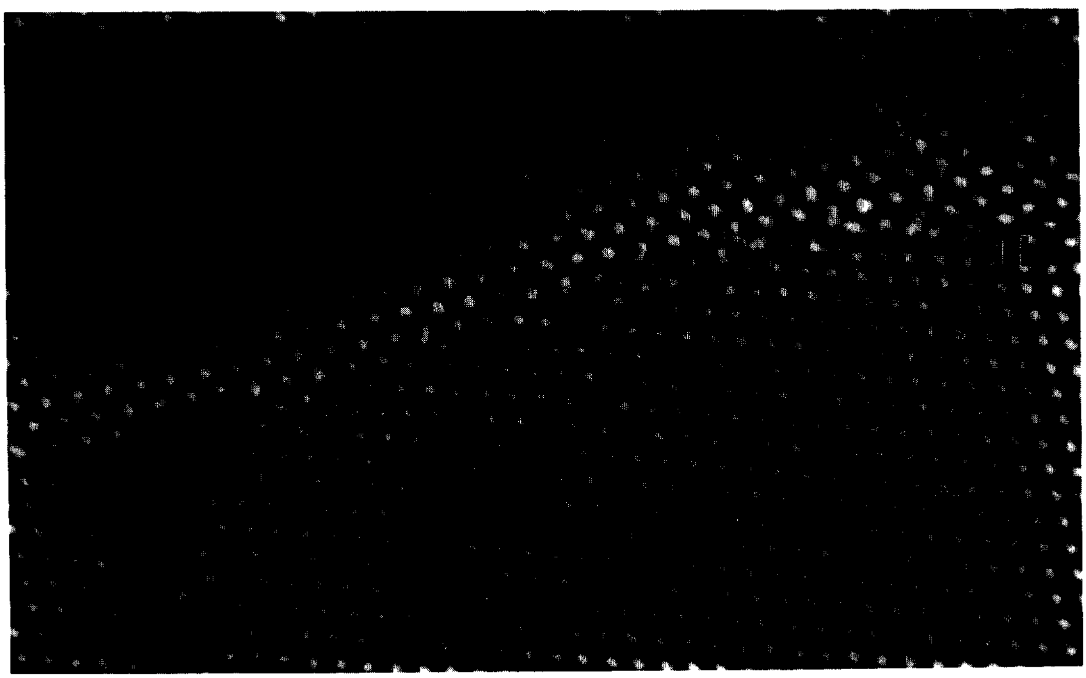

Fig 4 HREM image with incident beam parallel to $\{111\}$ plane of Si fiber revealing an asymmetric $\Sigma 9[110]/(\bar{1}12)$ twin boundary

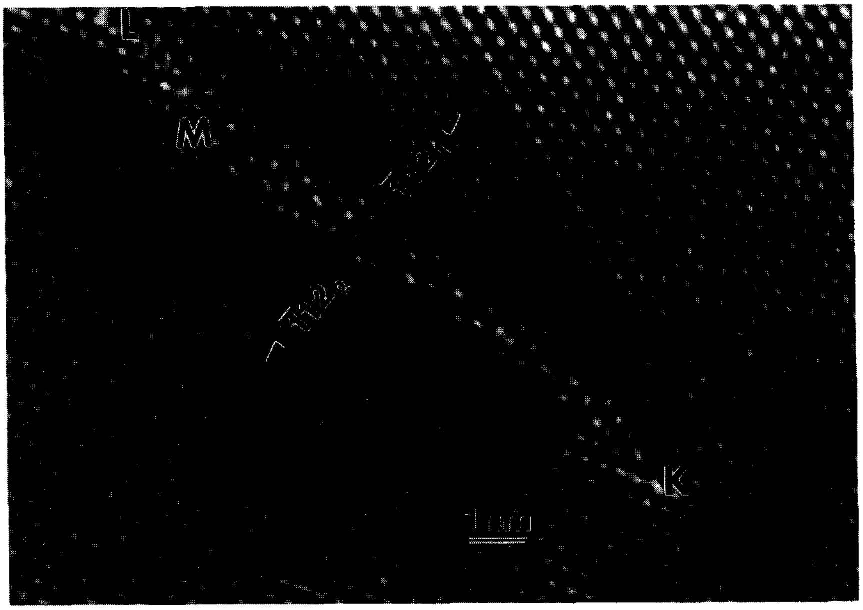

Fig 5 HREM image taken along [110] direction of Si fiber showing interaction between two cozonal and nonparallel $\Sigma 3[110]/\{111\}$ twin interfaces resulting in an asymmetric $\Sigma 3[110]/(\bar{1}12)$ grain boundary

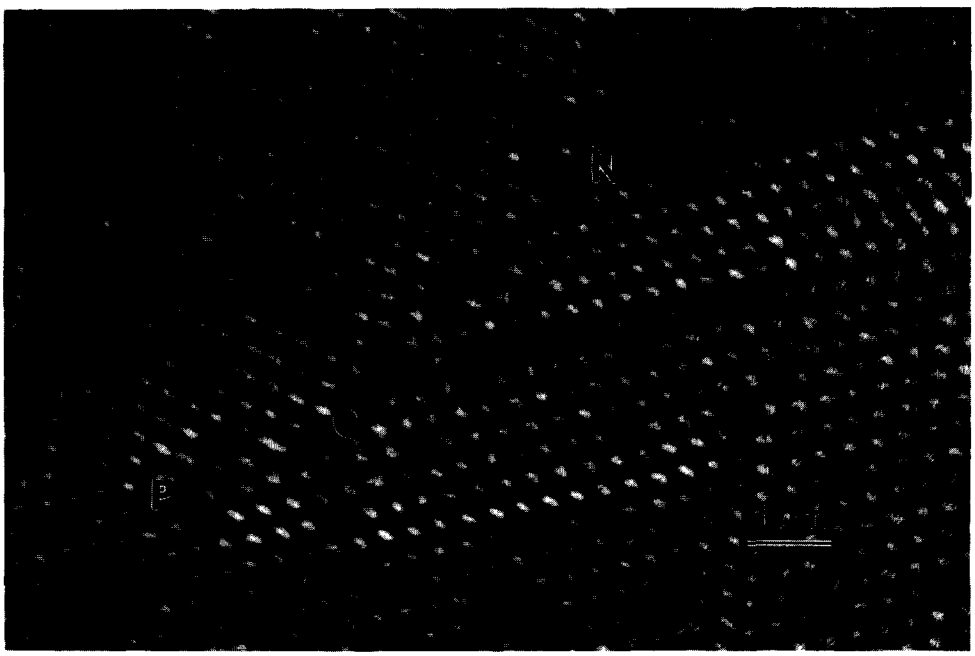

Fig 6 HREM image along [110] direction of Si fiber showing interaction between two cozonal nonparallel $\Sigma 3[110]/\{111\}$ twin interfaces resulting in an asymmetric $\Sigma 9[110]/(\bar{1}12)$ grain boundary

plane parallel to $\{111\}_1$ and $\{331\}_2$, whereas the segment between positions I and J has a boundary plane approximately parallel to $\{112\}_1$ and $\{441\}_2$

In addition to $\Sigma 3$ and $\Sigma 9$ twin boundaries, the high-resolution electron microscopy of these silicon fibers also revealed a number of interactions between various $\Sigma 3\langle 110\rangle/\{111\}$ twin boundaries resulting in the formation of $\Sigma 3\langle 110\rangle/\{112\}$ and $\Sigma 9\langle 110\rangle/\{112\}$ The position labelled K in fig 5 shows a location at which two $\Sigma 3\langle 110\rangle$ twins with grain boundary planes $(\bar{1}11)$ and $(1\bar{1}1)$ interact to produce a $\Sigma 3\langle 110\rangle/\{112\}$ boundary This $\Sigma 3\langle 110\rangle/\{112\}$ boundary is located between the positions marked K and L On average, the boundary appears symmetric about the common $\{112\}$, but careful inspection reveals that it displays asymmetry along certain segments One such segment between L and M is parallel to $\{113\}$ of the abutting crystals

Another reaction between two $\Sigma 3\langle 110\rangle/\{111\}$ twin boundaries producing a $\Sigma 9\langle 110\rangle$ boundary with symmetric and asymmetric segments occurs at the position marked N in the micrograph of fig 6 From N to O, the $\Sigma 9$ interface possesses a symmetric character with $\{112\}$ being the average grain boundary plane From O to P, the $\Sigma 9$ interface is too ill-defined to assign a specific grain boundary plane with any certainty The presence of a stacking fault terminating at the $\Sigma 9$ boundary complicates the morphological characterization of the interface

## 4. Discussion and conclusion

This preliminary study has focused on morphological changes in Si grain boundaries induced by the addition of Sr impurities This addition of Sr appears to promote considerable asymmetry in grain boundary plane orientation for $\Sigma 3\langle 110\rangle/\{111\}$, $\Sigma 3\langle 110\rangle/\{112\}$ and $\Sigma 9\langle 110\rangle/\{112\}$ boundaries, unlike previous studies [4–6] However, it seems likely that some of the differences originate from the preparation methods the earlier work used bicrystals prepared under very carefully controlled conditions to be close to the misorientation of interest Moreover, close inspection of our images also suggests that it will not be possible to characterize the structure of our complex grain boundaries in terms of simple structural units

**Acknowledgements**

This research was supported in part by the Facility for High Resolution Electron Microscopy in the Center for Solid State Science at Arizona State University, established with support from the National Science Foundation (Grant no DMR-89-13384) The authors also acknowledge financial support from the Department of Energy (Grant no DE-FG02-87ER45285)

## References

[1] G Henry, Rev Metall 56 (1959) 417
[2] G C Rellick, C G McMohan, Jr , H L Marcus and B W Palmberg, Met Trans 2 (1972) 1492
[3] G H Bishop, W H Hartt and G A Bruggeman, Acta Met 19 (1971) 37
[4] C D'Anterroche and A Bourret, Phil Mag A 49 (1984) 783
[5] A Bourret and G G Bacmann, Rev Phys Appl 22 (1987) 563
[6] M Elkajbaji, Doctoral Thesis, USTM, Grenoble, France, 1986
[7] M Shamsuzzoha and L M Hogan, J Cryst Growth 76 (1986) 429
[8] M Shamsuzzoha and L M Hogan, Phil Mag 54 (1986) 459